ELSEVIER

Biophysical Chemistry 80 (1999) 93–101

Biophysical Chemistry

www.elsevier.nl/locate/bpc

# Inverted hexagonal and cubic phases induced by α-tocopherol in fully hydrated dispersions of dilauroylphosphatidylethanolamine

Xiaoyuan Wang, Peter J. Quinn*

*Division of Life Sciences, King's College London, Campden Hill, London W8 7AH, UK*

Received 29 March 1999; received in revised form 27 April 1999; accepted 27 April 1999

**Abstract**

The effect of α-tocopherol on the thermotropic phase behaviour and structure of aqueous dispersions of 1,2-dilauoryl-*sn*-glycero-3-phosphoethanolamine was examined by synchrotron X-ray diffraction. The pure phospholipid exhibited a lamellar gel to liquid–crystal phase transition at 30°C on heating at 3°C $min^{-1}$ between 10°C and 90°C. The transition was reversible with a temperature hysteresis of 0.3°C on cooling. At temperatures less than 10°C only lamellar gel phase of the pure phospholipid was seen in co-dispersions of up to 20 mol% α-tocopherol. The presence of 2.5 mol% α-tocopherol caused the appearance of inverted hexagonal phase at temperatures just below the main phase transition temperature that co-existed with the lamellar gel phase. The intensity of scattering from the hexagonal-II phase increased with increasing proportion of α-tocopherol in the mixture and in proportions greater than 10 mol% it persisted at temperatures above the main transition and co-existed with the lamellar liquid–crystal phase of the pure phospholipid. At higher temperatures all co-dispersions containing up to 15 mol% α-tocopherol showed the presence of cubic phases. These phases indexed a Pn3m or Pn3 space grouping. When the proportion of α-tocopherol was increased to 20 mol% the only non-lamellar phase observed was inverted hexagonal phase. This phase co-existed with lamellar gel and liquid–crystal phases of the pure phospholipid, but was the only phase present at temperatures $> 60$°C. The X-ray diffraction data were used to construct a partial phase diagram of the lipid mixture in excess water between 10° and 90°C and up to 20 mol% α-tocopherol in phospholipid. 

*Keywords:* α-Tocopherol; Vitamin E; Phosphatidylethanolamine; Bilayer dispersions; Membranes; X-Ray diffraction; Cubic phases

* Corresponding author. Tel.: +44-171-3334408; fax: +44-171-3334408.
*E-mail address:* p.quinn@kcl.ac.uk (P.J. Quinn)

0301-4622/99/$ - see front matter 
PII: S0301-4622(99)00063-0

## 1. Introduction

Phospholipid dispersions have frequently been used as models of biomembrane structure. Synthetic phospholipids with defined acyl chain composition undergo well-characterised thermotropic phase transitions and perturbation of these transitions is a useful method of investigating the mode of interaction of phospholipids with other membrane constituents. This approach has been used in the present study to determine how α-tocopherol is distributed in bilayers of dilauorylphosphatidylethanolamine in gel and fluid phases and to gain insight into the effect of α-tocopherol on the stability of phospholipid structures.

α-Tocopherol is a lipid-soluble vitamin which is distributed widely throughout the body where it is found primarily in cell membranes. The proportion of α-tocopherol:phospholipid varies from one subcellular membrane to another. In the rat liver, e.g. the ratio is 14.6 mmol $mol^{-1}$ phospholipid in lysosomal membranes with lesser amounts in mitochondria (1 mmol $mol^{-1}$ phospholipid) and endoplasmic reticulum (0.5 mmol $mol^{-1}$ phospholipid) [1]. The principle function of α-tocopherol is said to be its action as a lipid antioxidant in the prevention of free radical damage to unsaturated membrane lipids [2–6]. A secondary role is thought to be as a membrane stabilising agent which is achieved by the formation of complexes with lipids such as free fatty acids and lysophospholipids which would otherwise destroy membrane integrity through their detergent-like properties [7]. A general approach to probe the location and function of α-tocopherol in membranes has been to examine its interaction with phospholipids [8–12]. Recent X-ray diffraction and calorimetric studies of mixed aqueous dispersions of α-tocopherol and phosphatidylcholine [13] has provided evidence for the formation of complexes in both the gel and fluid phases of the phospholipid which have a stoichiometry of phospholipid:α-tocopherol of 10:1. These studies support other evidence that indicates α-tocopherol is not randomly distributed in phospholipid bilayer membranes [14,15] but tends to be associated into α-tocopherol-rich domains. The localisation of α-tocopherol in membranes has been the subject of a recent review [16].

While there have been a number of studies of the effect of α-tocopherol and its homologues on the phase behaviour of phosphatidycholines [17–19] there is less information about the influence on the phase behaviour of phosphatidylethanolamines. Ortiz et al. [20] have reported calorimetric studies of mixed aqueous dispersions with dilauorylphosphatidylethanolamine and found that increasing amounts of α-tocopherol caused a progressive decrease in the main endothermic phase transition of the phospholipid. The studies reported here use synchrotron X-ray diffraction methods to provide direct structural information on the dilauorylphosphatidylethanolamine: α-tocopherol system to compliment the earlier calorimetric data. The results have been used to construct a partial phase diagram of the binary lipid mixture at full hydration over the temperature range 10–90°C and up to 20 mol% α-tocopherol in phospholipid. It was found that the mixture exhibits phase separations and formation of a variety of non-lamellar phases which co-exist with gel and fluid phase bilayers of the pure phospholipid.

## 2. Materials and methods

1,2-dilauroyl-*sn*-glycero-3-phosphoethanolamine (DLPE) was purchased from Avanti Polar Lipids (Alabaster, AL) and α-tocopherol (99%) from Acros Organics (Geel, Belgium). The lipids were dissolved in chloroform and mixed in appropriate proportions to achieve the desired molar fractions (mol% = mole α-tocopherol × 100/(mole DLPE + mole α-tocopherol)) of 2.5, 5, 7.5, 10, 15 or 20 mol%. The solvent was evaporated under a stream of oxygen-free dry nitrogen and stored for 24 h under vacuum to remove any remaining traces of solvent. The lipid mixtures were hydrated at 80°C with 2.4 ml of a buffer consisting of 0.1 mM EDTA, 10 mM HEPES (pH 7.5), 100 mM NaCl $g^{-1}$ of lipid and dispersed by vigorous rotamixing until homogeneous disper-

sions were obtained. The lipid dispersions were stored at 0–4°C until required for examination.

Synchrotron X-ray diffraction experiments were performed at station 8.2 of the Daresbury Synchrotron Radiation Laboratory, UK using a monochromatic (0.15405 nm) focused X-ray beam. The beam-line can generate a flux of $4 \times 10^{10}$ photons $s^{-1}$ with a focal spot size: 0.3 mm in height and 3 mm wide. A combined multi-wire quadrant detector to measure small-angle (0.1–3°) X-ray scattering (SAXS) intensity and an INEL curved linear-wire detector (Instrument Electronique, France) to measure wide-angle (4–25°) X-ray scattering (WAXS) was used. Details of the station set-up have been published elsewhere [21]. Samples were mounted in a slot ($1 \times 5$ mm) cut in a 1 mm thick copper plate that was sandwiched between a pair of thin mica sheets. The sandwich was clamped directly onto a silver block of a cryomicroscope stage (Linkam Scientific Instruments Ltd., Tadworth, UK). The temperature of the stage could be controlled to within $\pm 0.1$°C and the temperature of the sample was monitored by a thermocouple inserted into the dispersed lipid. Temperature scans in heating and cooling modes were performed at 3°C $min^{-1}$ over a temperature range 10–90°C. Samples were heated to 90°C prior to recording the first cooling scan to minimise exposure of the sample to the X-ray beam. X-ray scattering intensity data were acquired in 400 consecutive time frames and analysed using the OTOKO software programme developed at EMBL, Hamburg, Germany [22]. X-ray scattering intensities from the quadrant detector were corrected for fluctuations in beam intensity monitored by an ion chamber mounted on the incident beam and detector response recorded off-line using a $^{55}$Fe source. Spacial calibrations of the detector were performed using wet rat-tail collagen ($d = 67$ nm) [23]. The scattering intensity data recorded by the INEL detector was corrected for scattering from an empty cell and spacial calibrations were established from high-density polyethylene (0.4166, 0.3780, 0.3014 nm) [24]. The reciprocal spacing $S = 1/d = 2\sin(\theta)/\lambda$, where $d$, $\lambda$, $\theta$ are the repeat distance, X-ray wavelength and the diffraction angle, respectively.

## 3. Results

The phase behaviour and structural transitions that take place in fully hydrated dispersions of DLPE were examined by synchrotron X-ray diffraction methods and compared with dispersions of phospholipid containing varying amounts of α-tocopherol to determine the mode of interaction between the two lipids. Initial studies were performed on the pure phospholipid and plots of X-ray diffraction patterns recorded during a heating scan from 10°C to 90°C at 3°C $min^{-1}$ are presented in Fig. 1. The gel phase at 26°C is characterised by a lamellar repeat spacing of 5.07 nm with a single sharp symmetrical reflection at 0.422 nm indicating hexagonal packing of the acyl chains oriented vertically with respect to the bilayer plane. The liquid–crystal lamellae have a repeat spacing of 4.48 nm at 46°C and a broad wide-angle diffraction band centred at 0.45 nm typical of disordered hydrocarbon chains. The structural parameters are in good agreement with those reported by Seddon et al. [25]. It can be seen that the phospholipid undergoes a two-state transition from a lamellar gel to liquid–crystal phase transition ($L_\beta \rightarrow L_\alpha$) centred at 30.2°C in which there is co-existence of the initial and final states in the region of the transition with no detectable intermediate phases. A cooling scan performed immediately after the heating scan (data not given) showed that the transition was essentially reversible with a temperature hysteresis of about 0.3°C in the structural transitions.

Codispersions of DLPE with up to 20 mol% α-tocopherol consist of a single lamellar phase at temperatures $< 10$°C with a repeat spacing identical with that of the pure phospholipid. Heating these co-dispersions causes the appearance of additional phases presumably due to the formation of phospholipid domains enriched with α-tocopherol. This effect is illustrated in Fig. 2 which shows SAXS patterns recorded in DLPE co-dispersed with either 2.5, 5 or 10 mol% α-tocopherol during heating scans from 10° to 90°C at 3°C $min^{-1}$. Additional peaks appear in the scattering pattern at temperatures lower than the main gel to liquid–crystal phase transition of the phospholipid evidenced by the persistence of the

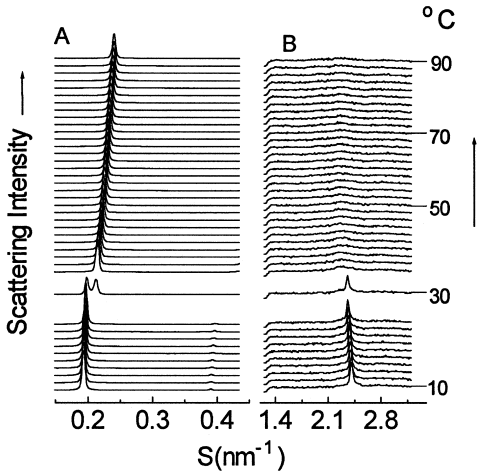


Fig. 1. Plots of successive X-ray scattering intensity profiles vs. reciprocal spacing of a fully hydrated dispersion of DLPE in the small-angle (A) and wide-angle region (B) recorded during heating from 10° to 90°C at 3°C min$^{-1}$. Each diffraction pattern represents scattering accumulated in 20 s. The temperature scale in the region of the transition is expanded to show co-existence of lamellar gel and liquid–crystal phases.

sharp wide-angle reflection at 0.422 nm. The diffraction maxima of the new SAXS peaks are in a ratio of $1:1/\sqrt{3}:1/\sqrt{4}$ and are assigned to an inverted hexagonal phase. The intensity of the scattering from the non-lamellar phase is directly related to the amount of α-tocopherol in the mixture at any particular temperature. This is illustrated in Fig. 3 which shows static diffraction patterns of co-dispersions of DLPE with different proportions of α-tocopherol recorded at 20°C. The repeat spacing of the lamellar gel phase that co-exists with the inverted hexagonal phase is indistinguishable from that of the pure phospholipid. Evidence for the formation of hexagonal-II phase can be seen in co-dispersions containing only 2.5 mol% α-tocopherol and suggests that the formation of hexagonal-II phase is due to enrichment of phospholipid bilayers with α-tocopherol.

The intensity of scattering observed from the hexagonal-II phase decreases markedly at a temperature co-inciding with the main transition temperature of the pure phospholipid. Heating mixed dispersions to temperatures greater than 60°C causes the appearance of additional peaks in the SAXS patterns that indicate the presence of cubic phases co-existing with the liquid–crystal lamellar phase. The repeat spacing of the lamellar phase is almost identical to that of the pure phospholipid suggesting that α-tocopherol is phase separated into the non-lamellar phases. These non-lamellar phases are clearly evident in mixed dispersions containing 2.5 mol% α-tocopherol further supporting the notion that α-tocopherol is largely excluded from bilayers of pure DLPE. The phase transition sequence on heating mixed dispersions of DLPE containing 10 mol% α-tocopherol is in the order: $L_\beta \rightarrow L_\beta + H_{II} \rightarrow L_\alpha + H_{II} \rightarrow L_\alpha + Q \rightarrow Q$ (Fig. 2c).

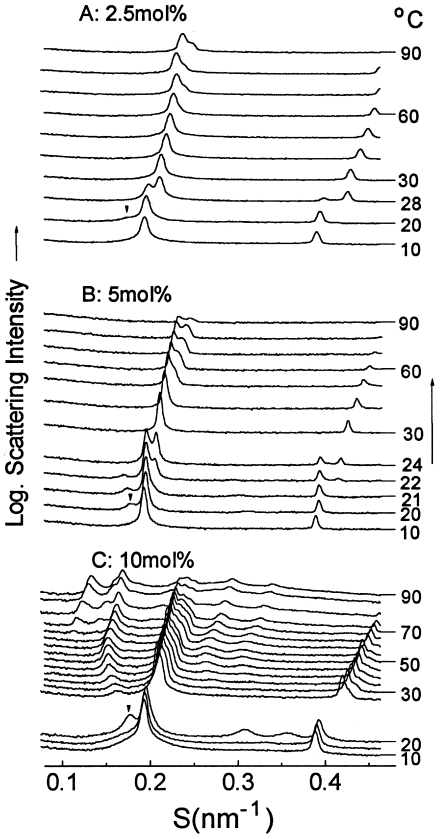


Fig. 2. Plots of X-ray scattering intensity profiles versus reciprocal spacing in the small-angle region of fully hydrated co-dispersions of (A) 2.5 mol%, (B) 5 mol% and (C) 10 mol% α-tocopherol in DLPE recorded during heating from 10° to 90°C at 3°C min$^{-1}$. Each diffraction pattern represents scattering accumulated in 20 s. First order diffraction maxima of the inverted hexagonal phase at 20°C are indicated by arrows.

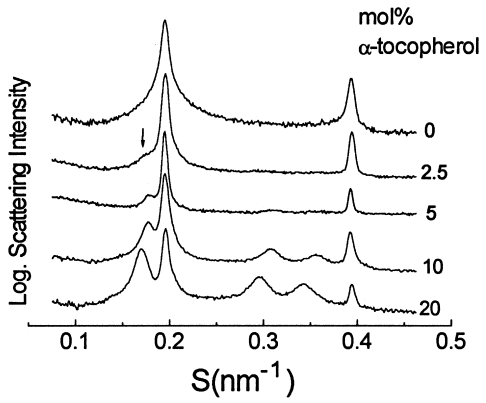


Fig. 3. Plots of successive X-ray scattering intensity profiles in the small-angle region vs. reciprocal spacing of co-dispersions of DLPE containing different concentrations of α-tocopherol at 20°C. The profiles were plotted on a logarithmic scale to accentuate the minor bands. The proportion of α-tocopherol in the dispersion is indicated on the respective diffraction pattern.

To identify the space group of the cubic phase a series of static X-ray diffraction experiments were performed. The results are presented in Fig. 4, which shows static diffraction patterns of mixtures containing 7.5, 10 and 15 mol% recorded at designated temperatures. It can be seen that cubic phases begin to dominate the diffraction patterns at 90°C in the mixture containing 7.5 mol% α-tocopherol (Fig. 4A), and represent the only phase at 99°C in the mixture containing 10 mol% α-tocopherol (Fig. 4B). An analysis of the diffraction patterns observed at 99°C in the co-dispersion containing 10 mol% α-tocopherol is presented in Fig. 5. The initial phase formed on heating to this temperature show scattering maxima which can be indexed to the Pn3m or Pn3 space group by nine diffraction bands in a ratio of $1/\sqrt{2}:1/\sqrt{3}:1/\sqrt{4}:1/\sqrt{6}:1/\sqrt{8}:1/\sqrt{9}:1/\sqrt{10}:1/\sqrt{12}:1/\sqrt{14}$. The positions of diffraction peaks of a Pn3m cubic lattice that are indexed (hkl) show that reciprocal spacings (S) vs. $(h^2 + k^2 + l^2)^{1/2}$ for hkl indices fall on a straight line passing through the origin. The lattice constant a = 10.18 ± 0.01 nm. It is noteworthy that in the mixture containing 15 mol% α-tocopherol, the Pn3m phase already dominates the diffraction pattern at 81°C and completely replaces the $L_\alpha$ phase at 92°C; there was no evidence of any transformation of this cubic space group even after heating to 101°C (Fig. 4C). Crystallographic data of the cubic phase shown in Fig. 4 is collated in Table 1.

Mixed aqueous dispersions of DLPE containing more than 15 mol% α-tocopherol showed no evidence of formation of cubic phases. This can be seen in Fig. 6 which shows plots of successive X-ray scattering intensity profiles recorded during heating a fully hydrated co-dispersion of DLPE containing 20 mol% α-tocopherol from 10° to 90°C at 3°C min$^{-1}$. An inverted hexagonal phase first appears at 16°C. The non-lamellar phase co-exists, firstly with $L_\beta$ phase and then with $L_\alpha$ phase of DLPE after the main transition at 21.3°C. The main transition of DLPE was established both by a change in lamellar repeat spacing (Fig. 6A) with evidence of phase co-existence in the transition region and replacement of the single symmetrical diffraction peak at 0.42 nm with a broad band centred at a spacing of 0.45 nm (Fig. 6B). The scattering intensity of the inverted hexagonal phase increased at the expense of the $L_\alpha$

Table 1
Reciprocal spacings (nm$^{-1}$) of diffraction peaks of the cubic phase observed in the co-dispersions of DLPE and α-tocopherol

| (hkl) of Pn3m | (110) | (111) | (200) | (211) | (220) | (221) | (310) | (222) |
|---|---|---|---|---|---|---|---|---|
| 7.5%, 90°C | 0.123 | 0.150 | | 0.210 | 0.248 | 0.256 | | |
| 7.5%, 100°C | 0.142 | 0.168 | | 0.241 | 0.284 | | | |
| 10%, 75°C | 0.116 | 0.142 | | | 0.235 | | | |
| 10%, 99°C | 0.140 | 0.172 | 0.198 | 0.243 | 0.280 | 0.299 | 0.314 | 0.346 |
| 15%, 81°C | 0.129 | 0.160 | 0.182 | 0.223 | 0.258 | 0.281 | | |
| 15%, 92°C | 0.140 | 0.170 | 0.197 | 0.240 | 0.280 | 0.296 | 0.304 | 0.340 |
| 15%, 101°C | 0.142 | 0.173 | 0.203 | 0.247 | 0.287 | 0.302 | 0.310 | 0.348 |

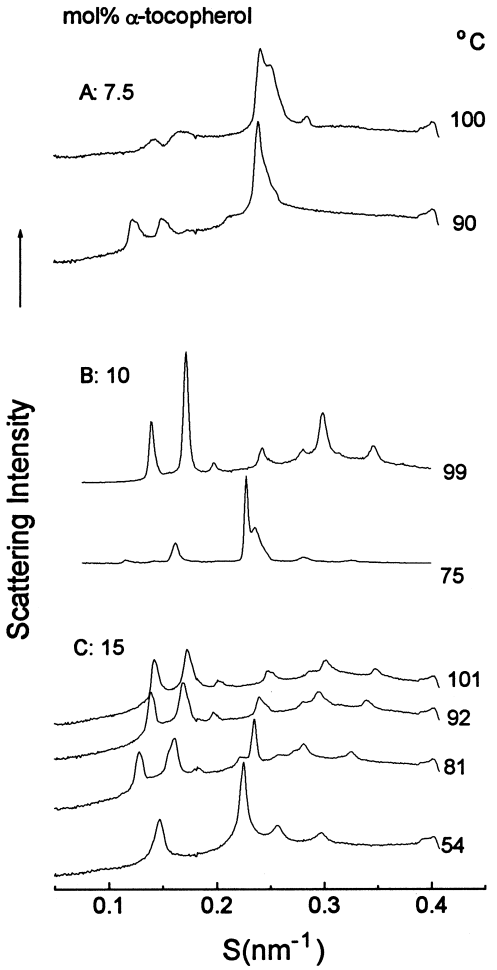


Fig. 4. Static small-angle X-ray scattering intensity profiles vs. reciprocal spacing of fully hydrated co-dispersions of (A) 7.5 mol%, (B) 10 mol% and (C) 15 mol% α-tocopherol in DLPE at designated temperatures. Each diffraction pattern represents scattering accumulated in 5 min.

phase with increasing temperature until the latter phase was completely replaced at 64°C (Fig. 6A).

To determine the effect of α-tocopherol on the main gel to liquid–crystal phase transition of DLPE an analysis of the temperature dependence of the scattering intensity of the wide-angle peak was undertaken. The relationship between relative integrated X-ray scattering intensity of the wide-angle bands of DLPE containing varying amounts of α-tocopherol are plotted as a function of temperature in Fig. 7a. This shows that

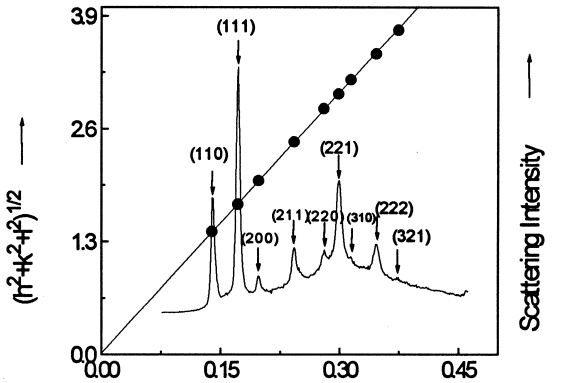


Fig. 5. Static small-angle X-ray diffraction patterns of a co-dispersion of DLPE containing 10 mol% α-tocopherol recorded at 99°C. Arrows indicate the predicted locations of diffraction peaks of a Pn3m cubic lattice that are indexed (hkl). The reciprocal spacings (S) vs. $(h^2 + k^2 + l^2)^{1/2}$ for hkl indices fall on a straight line from which a lattice constant, $a = 10.18 \pm 0.01$ nm, is obtained from the reciprocal slope.

cooperativity of the transition, as judged by the temperature range over which the chain melting occurs, decreases with increasing amounts of α-

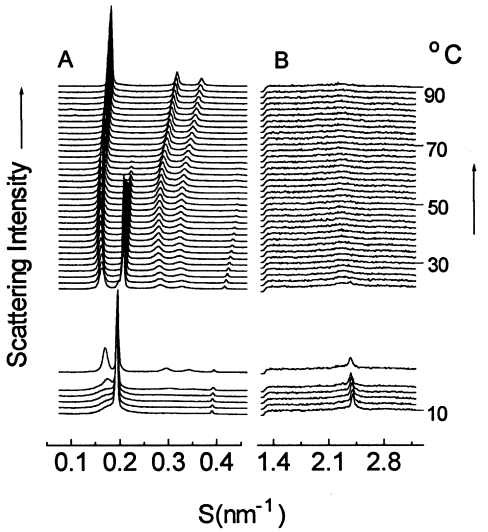


Fig. 6. Plots of successive X-ray scattering intensity profiles versus reciprocal spacing of a fully hydrated co-dispersion of DLPE containing 20 mol% α-tocopherol in the small-angle (A) and wide-angle regions (B) recorded during heating from 10° to 90°C at 3°C $min^{-1}$. Each diffraction pattern represents scattering accumulated in 20 s. The temperature scale is expanded in the region of the gel to liquid–crystal transition to show details of the co-existing phases.

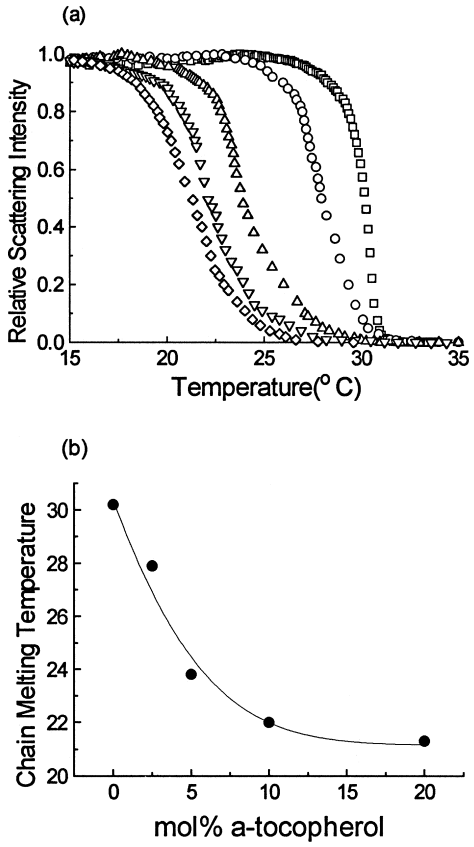


Fig. 7. (a) Temperature dependence of normalised X-ray scattering intensity of wide-angle peaks of mixed aqueous dispersions of DLPE containing (□) 0; (○);2.5; (△) 5; (▽) 10; (◇) 20 mol% α-tocopherol recorded during heating through the gel to liquid–crystal phase transition. (b) Effect of α-tocopherol on the temperature of the main transition of DLPE.

tocopherol in the phospholipid. A plot of the temperature of the mid-point of the transition against the amount of α-tocopherol in the dispersion is presented in Fig. 7b. It is clear that α-tocopherol causes a decrease in the chain melting transition of the phospholipid.

## 4. Discussion

Knowledge of the location of α-tocopherol in membranes is essential to understand the mechanisms attributed to the function of the vitamin. While studies of the distribution of α-tocopherol within biological membranes are few, there is a wealth of information about the orientation and arrangement of α-tocopherol in phospholipid model membranes. The majority of these studies have been performed using bilayer-forming phospholipids, usually phosphatidylcholines. The conclusion from these studies are that α-tocopherol is interpolated between the phospholipid molecules where it rotates about its axis perpendicular to the plane of the bilayer [26–28]. There is also clear evidence of domain formation with regions of the bilayer enriched with α-tocopherol, which appears to be influenced by the acyl chain composition of the phospholipid [8,29].

The present data confirm recent reports that the distribution of α-tocopherol in non-bilayer forming phosphatidylethanolamines is different from the phosphatidylcholines [20,30]. In particular, it is clear that α-tocopherol does not form a stable bilayer with phosphatidylethanolamines in the gel phase. The low-temperature equilibrium phases tend to be one of two lamellar crystal phases which are formed by the penetration of α-tocopherol from aggregates of pure α-tocopherol phase separated from the lamellar gel phase of the pure phospholipid [31]. These lamellar crystal phases have a stoichiometry of phospholipid:α-tocopherol of approximately 4:1 and the complex co-exists with the lamellar gel phase of the pure phospholipid. Upon heating the lamellar crystal phase transforms directly to inverted hexagonal phase or, as seen in the present experiments, the phase separated α-tocopherol penetrates into the gel phase phospholipid to form a complex in inverted hexagonal arrangement which co-exists with bilayers of pure gel phase phospholipid. The transition from bilayer to non-bilayer phase may correspond with the first enthalpy change during heating of mixed aqueous dispersions of phosphatidylethanolamines and α-tocopherol reported by Ortiz et al [20]. The second endothermic peak in calorimetric heating scans could correspond to the lamellar gel to liquid–crystal phase transition of the pure phospholipid phase. The present results confirm that the temperature of the main transition decreases with increasing proportion of α-tocopherol in the mixture.

At temperatures above the main phase transition the inverted hexagonal phase consisting of α-tocopherol and phospholipid in defined stoichiometry co-exists with fluid phase bilayers of pure phospholipid. With mixtures of α-tocopherol and dilauorylphosphatidylethanolamine a high temperature cubic phase is formed. The cubic phase indexes to a Pn3m cubic lattice. Cubic phases of the Pn3m type have only been seen in saturated phosphatidylethanolamine:α-tocopherol mixtures in the case of the dimyristoyl molecular species only in the presence of approximately 10 mol% α-tocopherol [30]. In all other cases the hexagonal-II phase co-existing with pure phosphatidylethanolamine in the liquid–crystal state is the preferred phase. Clearly short chain length favours cubic phase formation.

The diffraction data have been used to construct a partial phase diagram of fully hydrated mixtures of dilauorylphosphatidylethanolamine: α-tocopherol over the range 0–20 mol% α-tocopherol and temperatures between 10° and 90°C. The diagram is shown in Fig. 8. The structural parameters of all lamellar phases are almost identical to that of the pure phospholipid and a priori is taken to be evidence that α-tocopherol is not miscible with the phase. The pure phospholipid exists only in lamellar phase over the temperature range covered by the phase diagram and the non-lamellar phases are comprised of α-tocopherol and phospholipid in defined stoichiometry. Of interest is the formation of cubic phase at high temperatures in the presence of $< 15$ mol% α-tocopherol, however, the preference for inverted hexagonal phase at higher proportions of α-tocopherol in phospholipid.

The implications of the present results on the stability of cell membranes is worthy of consideration. Formation of lamellar complexes of α-tocopherol with phosphatidylcholines would tend to have a stabilising effect on membranes. The phase separation of α-tocopherol from bilayer arrangements of phosphatidylethanolamines and the strong tendency to form non-bilayer complexes with phosphatidylethanolamines would strongly destabilise cell membranes. Membrane destabilisation is required for processes like fusion and protein translocation across membranes

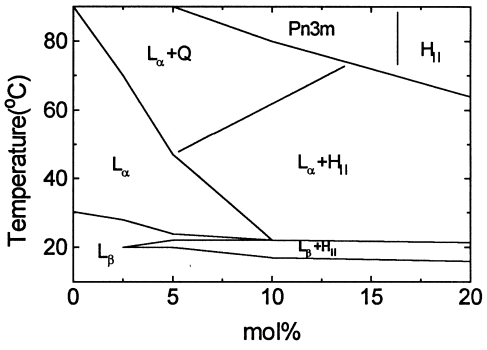


Fig. 8. A partial phase diagram of the system α-tocopherol/DLPE in excess water. The assignment of phases are indicated in respective regions of the diagram.

[32,33] and α-tocopherol could be involved in mediation of these events. The factors which govern the distribution of α-tocopherol in biological membranes and which are believed to be responsible for the putative membrane stabilising function of the vitamin have yet to be fully appreciated.

## Acknowledgements

Financial support and beamtime for the experiments was awarded by the Daresbury Laboratory. X.W. is supported by KC Wong Education Foundation Studentship.

## References

[1] J.L. Buttriss, A.T. Diplock, Biochim. Biophys. Acta 963 (1988) 61.
[2] M. Scarpa, A. Rigo, M. Maiorino, F. Ursini, C. Gregolin, Biochim. Biophys. Acta 801 (1984) 215.
[3] B. Halliwell, J.M.C. Gutteridge, Free radicals in biology and medicine, Clarendon Press, Oxford, 1991.
[4] H. Sies, Oxidative stress: oxidants and antioxidants, Academic Press, San Diego, 1991.
[5] D.C. Liebler, Crit. Rev. Toxicol. 23 (1993) 147.
[6] K. Fukuzawa, K. Matsuura, A. Tokumura, A. Suzuki, J. Terao, Free Radical Biol. Med. 22 (1997) 923.
[7] V.E. Kagan, Ann. NY. Acad. Sci. 570 (1988) 120.
[8] M. Sanchez-Migallon, F.J. Aranda, J.C. Gomez-Fernandez, Biochim. Biophys. Acta 1279 (1996) 251.
[9] M. Sanchez-Migallon, F.J. Aranda, J.C. Gomez-Fernandez, Biochim. Biophys. Acta 1281 (1996) 23.

[10] J. Salgado, J. Villalain, J.C. Gomez-Fernandez, Biochim. Biophys. Acta 1239 (1995) 213.
[11] V. Micol, F.J. Aranda, J. Villalain, J.C. Gomez-Fernandez, Biochim. Biophys. Acta 1022 (1990) 194.
[12] T. Lefevre, M. Picquart, Biospectroscopy 2 (1996) 391.
[13] P.J. Quinn, Eur. J. Biochem. 233 (1995) 916.
[14] V.E. Kagan, P.J. Quinn, Eur. J. Biochem. 171 (1988) 661.
[15] F.J. Aranda, A Coutinho, M.N. Berberan-Santos, M.J.E. Prieto, J.C. Gomez-Fernandez, Biochim. Biophys. Acta 985 (1989) 26.
[16] P.J. Quinn, Subcell. Biochem. 30 (1998) 319.
[17] J.B. Massey, H.S. She, H.J. Pownall, Biochem. Biophys. Res. Commun. 106 (1982) 842.
[18] B. DeKruijff, P.W.M. VanDijck, R.A. Demel, A. Schuijff, F. Brants, L.L.M. VanDeenen, Biochim. Biophys. Acta 356 (1974) 1.
[19] J. Villalain, F.J. Aranda, J.C. Gomez-Fernandez, Eur. J. Biochem. 158 (1986) 141.
[20] A. Ortiz, F.J. Aranda, J.C. Gomez-Fernandez, Biochim. Biophys. Acta 898 (1987) 214.
[21] P.J. Quinn, J. Appl. Cryst. 30 (1997) 733.
[22] C. Boulin, R. Kempf, M.H.J. Koch, S.M. McLauchlin, Nuc. Instr. Methods Phys. Res. A249 (1986) 399.
[23] A. Bigi, N. Roveri, in: S. Ebashi, M. Koch, E. Rubenstein (Eds.), Fibre Diffraction: Collagen (Handbook on Synchrotron Research, 4, Elsevier Science Publishers B.V., The Netherlands, 1991, p. 25.
[24] E.J. Addink, J. Beintema, Polymer 2 (1961) 185.
[25] J.M. Seddon, K. Harlos, D. Marsh, J. Biol. Chem. 258 (1983) 3850.
[26] S. Urano, M. Iida, I. Otani, M. Matsuo, Biochem. Biophys. Res. Commun. 146 (1987) 1413.
[27] J. Salgado, J. Villalain, J.C. Gomez-Fernandez, Eur. J. Biochem. 22 (1993) 151.
[28] Y. Suzuki, M. Tsuchiya, S.R. Wassall, G. Govil, V.E. Kagan, L. Packer, Biochemistry 32 (1993) 10692.
[29] W. Stillwell, T. Dallman, A.C. Dumanual, F.T. Crump, L.J. Jenski, Biochemistry 35 (1996) 13353.
[30] X. Wang, H. Takahashi, I. Hatta, P.J. Quinn, Biochim. Biophys. Acta 1418 (1999) 335.
[31] X. Wang, P.J. Quinn, Eur. J. Biochem., in press.
[32] J.M. Seddon, Biochim. Biophys. Acta 1031 (1990) 1.
[33] B. DeKruijff, Nature 386 (1997) 129.